







Metasurface design for the generation of an arbitrary assembly of different polarization statesYa-Jun Gao ¹, Ziyu Wang ¹, Wenjie Tang,¹ Xiang Xiong,¹ Zhenghan Wang,¹ Fei Chen ¹,
Ru-Wen Peng ^{1,*} and Mu Wang ^{1,2,†}¹*National Laboratory of Solid State Microstructures, School of Physics, and Collaborative Innovation Center of Advanced Microstructures, Nanjing University, Nanjing 210093, China*²*American Physical Society, Ridge, New York 11961, USA* (Received 14 April 2021; revised 5 July 2021; accepted 11 August 2021; published 10 September 2021)

Manipulation of polarization states with metasurfaces is a compelling approach for on-chip photonics and portable information processing. Yet it remains challenging to generate different types of polarization states with a single piece of a metasurface. This paper demonstrates a metasurface to resolve this issue, which is made of L-shaped resonators with different geometrical sizes. Each resonator diffracts a right- or left-handed circularly polarized state with an additional geometrical-scaling-induced phase. The type of polarization state of each diffracted beam is determined by the enantiomorphism, size, and spatial sequence of the resonators in the unit cell. The number of the beams is modulated by the geometry and separation of the resonators. We provide examples to illustrate how to achieve the specific number of diffracted beams with the desired polarization states in experiments. We suggest that this strategy can be applied for integrated photonics and portable quantum information processing.

DOI: [10.1103/PhysRevB.104.125419](https://doi.org/10.1103/PhysRevB.104.125419)**I. INTRODUCTION**

Polarization is an important feature of the electromagnetic wave in addition to its amplitude, phase, and propagation direction. It plays an important role in ellipsometry [1], stress detection [2], optical mineralogy [3], stellar spectroscopy [4], display technology [5], and antenna technology [6], etc. Recently, polarization management becomes an even more important issue in quantum information and integrated photonics. For example, photons are encoded with multiple different polarization states to guarantee the secure quantum key distribution [7–10]. On the other hand, nowadays, polarization generation and conversion are usually accomplished by the combination of birefringent prisms and beam splitters [11–13]. Usually, these optical elements are bulky and heavy, and are difficult to incorporate into an on-chip device. The development of metasurface-based polarization management is a promising approach to miniaturize the conventional optical elements [14,15].

A metasurface is an artificial microstructure made of arrays of dielectric or metallic subwavelength resonators [14,16]. The anisotropic resonators with a single symmetrical axis, such as “V” or “L” shapes, can be designed to convey the distinct phases to the light beams polarized in two orthogonal directions. By modulating the phase distribution, the metasurface can manipulate the amplitude, phase, polarization, and wave vector of electromagnetic waves [17–35]. As a light beam passes through an isotropic dielectric material, an add-up phase is built, which is determined by the

refractive index of the material and the physical propagation distance. This phase is usually termed the dynamic phase. Another phase in the light-matter interaction is the geometric phase, which arises from either the intrinsic atomic/molecular anisotropy of the material itself or the anisotropic scattering of the subwavelength building blocks. This additional phase is proportional to an effective optic axis orientation or related to the shape of anisotropic scattering structures, or both [36]. The geometric phase was first introduced in interference theory by Pancharatnam in 1956 [37] and subsequently extended to quantum-mechanical systems by Berry in 1984 [38]. Nowadays, people usually use the Pancharatnam-Berry (P-B) phase to describe the phase modulations induced by the rotation of a microstructure in optics [39–49]. The other source of the geometric phase, which is contributed by the inflation/contraction of the interacted microstructure, can be termed as the geometrical-scaling-induced phase (GSI phase) [50] in contrast to the rotation-induced phase (P-B phase). In this paper, we focus on the effects of the GSI phase.

When an electromagnetic wave illuminates on the metasurface composed of periodic resonator arrays, the resonators will be excited. Each resonator radiates with a specific phase modulation determined by its physical properties. The interference of the radiations from these resonators leads to the diffraction beams. Consider a general scenario where the metasurface comprises an array of unit cells ($N_1 \times N_2$). Each unit cell consists of $Q_1 \times Q_2$ resonators. Suppose $|P_{j,k}\rangle$ denote the radiation field of each resonator ($P_{j,k}$ with $j = 1, 2, \dots, Q_1$; $k = 1, 2, \dots, Q_2$) in the unit cell. When a plane wave shines on the metasurface, according to Ref. [51], the (n,m) order of the diffraction field of the metasurface can be

* rwpeng@nju.edu.cn† muwang@nju.edu.cn

expressed as

$$\begin{aligned}
 |k_n, k_m\rangle &= \frac{1}{D_x D_y} \sum_{j=1}^{Q_1} \sum_{k=1}^{Q_2} \left\{ |P_{j,k}\rangle \right. \\
 &\quad \times \int_{(j-\frac{Q_1}{2}-1)\frac{D_x}{Q_1}}^{(j-\frac{Q_1}{2})\frac{D_x}{Q_1}} e^{-i\frac{2\pi n}{D_x}x} dx \int_{(k-\frac{Q_2}{2}-1)\frac{D_y}{Q_2}}^{(k-\frac{Q_2}{2})\frac{D_y}{Q_2}} e^{-i\frac{2\pi m}{D_y}y} dy \left. \right\} \\
 &= a_{n,m} \sum_{j=1}^{Q_1} \sum_{k=1}^{Q_2} |P_{j,k}\rangle e^{-i2\pi(\frac{nj}{Q_1} + \frac{mk}{Q_2})}, \quad (1)
 \end{aligned}$$

where $D_x(D_y)$ is the periodicity of unit cell in $x(y)$ direction, $k_n = \frac{2\pi}{\lambda} \sin \theta_x = \frac{2\pi n}{D_x}$, $k_m = \frac{2\pi}{\lambda} \sin \theta_y = \frac{2\pi m}{D_y}$. λ is the incident wavelength, m and n are either positive/negative integers or zero (the diffraction order). θ_x and θ_y are the diffraction angles. $a_{n,m}$ is the coefficient related to λ , D_x , D_y , m , and n .

Suppose the incident beam is expressed as $\alpha|x\rangle + \beta e^{i\eta}|y\rangle$, where α and β are respectively the amplitude of the x and y components of the incident beam, satisfying $|\alpha|^2 + |\beta|^2 = 1$. η is the phase difference between x and y components of the incident beam. The Jones vectors of horizontally linearly polarized (LP) state ($|x\rangle$) and vertically LP state ($|y\rangle$) are expressed as $\begin{bmatrix} 1 \\ 0 \end{bmatrix}$ and $\begin{bmatrix} 0 \\ 1 \end{bmatrix}$. The Jones vectors of the right-handed circularly polarized (RCP) state ($|R\rangle$) and left-handed circularly polarized (LCP) state ($|L\rangle$) are expressed respectively as $\frac{\sqrt{2}}{2}\begin{bmatrix} 1 \\ -i \end{bmatrix}$ and $\frac{\sqrt{2}}{2}\begin{bmatrix} 1 \\ i \end{bmatrix}$. The anisotropic resonator with a single symmetrical axis can be described by the Jones matrix as

$$\begin{aligned}
 J_{j,k} &= \begin{bmatrix} \cos \theta_{j,k} & -\sin \theta_{j,k} \\ \sin \theta_{j,k} & \cos \theta_{j,k} \end{bmatrix} \times \begin{bmatrix} e^{i\phi_{j,k}} & 0 \\ 0 & e^{i(\phi_{j,k} + \Delta\phi_{j,k})} \end{bmatrix} \\
 &\quad \times \begin{bmatrix} \cos \theta_{j,k} & \sin \theta_{j,k} \\ -\sin \theta_{j,k} & \cos \theta_{j,k} \end{bmatrix}, \quad (2)
 \end{aligned}$$

where $\theta_{j,k}$ is the rotation angle of the symmetrical axis of the resonator from the x axis, $\phi_{j,k}$ and $(\phi_{j,k} + \Delta\phi_{j,k})$ are the phase added by the resonator when the polarization of incident light is in parallel and in orthogonal with the symmetrical axis of the resonator, respectively. These phases are determined by the geometrical sizes of the resonator [14]. It follows that the electric field of the transmitted/reflected light from the resonator can be expressed as

$$\begin{aligned}
 |P_{j,k}\rangle &= J_{j,k}(\alpha|x\rangle + \beta e^{i\eta}|y\rangle) \\
 &= \frac{\sqrt{2}}{4} e^{i\phi_{j,k}} [(\alpha - \beta e^{i(\eta + \frac{\pi}{2})})(1 + e^{i\Delta\phi_{j,k}}) \\
 &\quad + (\alpha + \beta e^{i(\eta + \frac{\pi}{2})})(1 - e^{i\Delta\phi_{j,k}}) e^{-i2\theta_{j,k}}] |L\rangle \\
 &\quad + \frac{\sqrt{2}}{4} e^{i\phi_{j,k}} [(\alpha + \beta e^{i(\eta + \frac{\pi}{2})})(1 + e^{i\Delta\phi_{j,k}}) \\
 &\quad + (\alpha - \beta e^{i(\eta + \frac{\pi}{2})})(1 - e^{i\Delta\phi_{j,k}}) e^{i2\theta_{j,k}}] |R\rangle. \quad (3)
 \end{aligned}$$

Equation (3) indicates clearly that the radiation field is determined by the incident field (α , β , η), the rotation angle ($\theta_{j,k}$), and geometrical aspects of the resonator ($\phi_{j,k}$, $\Delta\phi_{j,k}$).

Suppose an x -polarized ($\alpha = 1$, $\beta = 0$) incident beam shines on a metasurface made of identical V-shaped (L-shaped) resonators orienting to different directions.

Each resonator is designed as a half-wave plate, with $\Delta\phi_{j,k} = \pi$, $\phi_{j,k} = \Psi$. In this case, the only variable in Eq. (3) is $\theta_{j,k}$. Equation (3) can be simplified as $|P_{j,k}\rangle = \frac{\sqrt{2}}{2} e^{i\Psi} [e^{i(-2\theta_{j,k})}|L\rangle + e^{i(2\theta_{j,k})}|R\rangle]$. The P-B phase added to the LCP component equals $-2\theta_{j,k}$, and that added to the RCP component is $2\theta_{j,k}$. This situation makes the RCP and LCP components strongly correlated in phase. Consider a scenario that the resonator within the unit cell is arbitrarily arranged, by taking $|P_{j,k}\rangle = \frac{\sqrt{2}}{2} e^{i\Psi} [e^{i(-2\theta_{j,k})}|L\rangle + e^{i(2\theta_{j,k})}|R\rangle]$ into Eq. (1), the concrete forms of the (n,m) order of the diffraction field $|k_n, k_m\rangle$ and the $(-n, -m)$ order of the diffraction field $|k_{-n}, k_{-m}\rangle$ are obtained. The constant prefactor $\frac{\sqrt{2}}{2} a_{n,m} e^{i\Psi}$ ($\frac{\sqrt{2}}{2} a_{-n,-m} e^{i\Psi}$) of $|k_n, k_m\rangle$ ($|k_{-n}, k_{-m}\rangle$) does not affect the polarization and can be taken as unity. It can be seen that $|k_n, k_m\rangle^* = |k_{-n}, k_{-m}\rangle$ is always satisfied, where the star in the superscript stands for the conjugate operation. This means that no matter how the resonators are arranged in the unit cell, the output beams of (n,m) and $(-n, -m)$ orders are always in conjugated states, i.e., they are a pair of conjugated elliptical polarized states or circularly polarized (CP) states, or pairs of LP states with the same polarization. We should emphasize that if the incident beam is y -polarized, we can obtain the same results. Therefore we conclude that the polarization states of the output beams of (n,m) and $(-n, -m)$ orders are always correlated. In other words, with the P-B phase, it is impossible to simultaneously generate an assembly of polarization states of different types.

To resolve the restriction in generating polarization states, several attempts have been made. Wu *et al.* proposed constructing a metasurface with six individual regions with different P-B phases to generate four LP states and two CP states [42]. Yet with this approach, the correlation of the diffracted LCP and RCP light resumes. Besides, the separated regions with different functionalities impose a much stricter requirement on the homogeneity of the intensity profile of the incident beam if an equal-intensity output is required. Recently, it has been reported that by changing both the geometrical size and the rotation angle of the resonators in a metasurface, the phase distribution of LCP and RCP at the interface can be separately controlled [52–56]. In Ref. [52], the resonator is so designed that $\Delta\phi_{j,k} = \pi$. In Eq. (3), the independent variables become $\theta_{j,k}$ and $\phi_{j,k}$. Suppose the incidence is RCP (LCP), Eq. (3) shows that the phase added up to the output LCP (RCP) is $(\phi_{j,k} - 2\theta_{j,k})$ ($(\phi_{j,k} + 2\theta_{j,k})$). Meanwhile, the add-up phase imposed on LCP and RCP components can be tuned separately, where $\phi_{j,k}$ is a parameter determined by the geometrical parameter of the resonator. In Ref. [55], the incidence is a CP state. There are three independent variables $\phi_{j,k}$, $\theta_{j,k}$ and $\Delta\phi_{j,k}$. If the incidence is an LCP state, based on Eq. (3), the phase of the LCP and RCP component of the radiation field are respectively $(\phi_{j,k} + \Delta\phi_{j,k}/2)$ and $(\phi_{j,k} + \Delta\phi_{j,k}/2 - \pi/2 + 2\theta_{j,k})$. The sum of the phases adding up to LCP and RCP components is not zero, and the functionalities of the output LCP and RCP components can be realized separately. In Refs. [52,55], despite the phase distribution of the output RCP and LCP can be separately tuned, it remains difficult to generate different types of polarization states in the output beams.

In Ref. [50], Gao *et al.* demonstrated a metasurface made of L-shaped resonators with different geometrical sizes and mirror-imaged counterparts. Each resonator satisfies $\Delta\phi_{j,k} = \pi/2$, $\theta_{j,k}$ is fixed as $\pi/4$ for the L-shaped resonator and as $3\pi/4$ for the mirror image of the L-shaped resonator. Hence the independent variable becomes $\phi_{j,k}$ only. It follows that for an x -polarized incidence, the radiated field from the resonator is either an LCP or an RCP state. The add-up phase to the output state $\phi_{j,k}$ is a GSI phase. With this approach, the phase distribution of output LCP and RCP states becomes completely independent. In this way, any assembly of different types of polarization states becomes possible with a single piece of metasurface.

However, in Ref. [50], the enumeration approach has been applied to select resonators to generate the desired polarization combination. Although this approach seems straightforward, practically, using parameter scans makes the whole process cumbersome and time-consuming. Here, with the matrix inversion approach, the construction of the unit cell becomes a concise, standard process. The desired structures can be more easily targeted.

In this paper, we demonstrate examples of the combination of different numbers and different types of polarization states diffracted from a metasurface simultaneously based on the GSI phase. Each resonator diffracts either RCP or LCP state in the unit cell with an add-up phase determined by its geometrical features. The interaction of the diffracted field from these resonators leads to multiple output beams. The output polarization state is determined by the enantiomorphism, size, and spatial sequence of the resonators within the unit cell. The number of the output diffraction beams can be accurately modulated by selecting the resonators and their separation.

More specifically, our metasurface is made of an array of symmetric L-shaped resonators with various arm lengths and widths, and their mirror images sitting on top of a SiO₂-gold-silicon substrate. By deliberately selecting the resonators within the unit cell based on matrix inversion, an assembly of LCP, RCP, and any orthogonal LP states is simultaneously generated. Further, the number of output beams can be controlled. By shrinking the periodicity of the unit cell, the number of the output beams can be reduced to two, with one beam in RCP/LCP, and the other in one of the LP (horizontally/vertically/ $\pm 45^\circ$) states, or two beams in LP (horizontally and vertically) states. By changing the spatial sequence of the resonators in the unit cell, it is even possible to generate only one CP/LP beam. These examples demonstrate the unique feature and powerful functionality of the metasurface based on the GSI phase designing.

II. PRINCIPLE OF THE METASURFACE DESIGN

Equation (1) describes the diffraction field from the metasurface made of an array of unit cells consisting of $Q_1 \times Q_2$ resonators. Here, we consider a special case, $Q_2 = 1$, and the periodicity of the unit cell in the y direction, D_y , satisfies $D_y < \lambda$, where λ is the incident wavelength. With this setup, there will be no diffraction in the y direction, so we focus on the contribution of the resonator assembly in the x direction only. The radiation field from each resonator (P_j with $j =$

$1, 2, \dots, Q_1$) is denoted as $|P_j\rangle$. By taking $Q_2 = 1$ in Eq. (1), the n th order of the diffraction field of the metasurface can be expressed as

$$|k_n\rangle = \frac{1}{D_x} \sum_{j=1}^{Q_1} \int_{(j-\frac{Q_1}{2}-1)\frac{D_x}{Q_1}}^{(j-\frac{Q_1}{2})\frac{D_x}{Q_1}} |P_j\rangle e^{-i\frac{2\pi n}{D_x}x} dx. \quad (4)$$

Based on Eq. (4), $|k_n\rangle$ and $|P_j\rangle$ can be connected by an $R_1 \times R_2$ matrix, \mathbf{A} , where R_1 is the number of the expected diffraction states, and R_2 is the number of the independent resonators in the unit cell. $|k_n\rangle$ and $|P_j\rangle$ are $R_1 \times 1$ and $R_2 \times 1$ column vectors, respectively. Equation (4) can be rewritten as $|k_n\rangle = \mathbf{A}|P_j\rangle$. Once $|k_n\rangle$ and \mathbf{A} are given, $|P_j\rangle$ can be obtained directly from $|P_j\rangle = \mathbf{A}^{-1}|k_n\rangle$. \mathbf{A} is a reversible matrix when $R_1 = R_2$, and its determinant should be nonzero.

In this paper, the resonators in the unit cell are designed as the symmetric L-shaped gold resonators sitting on top of a SiO₂-gold-silicon substrate [17]. The incident light shines on the metasurface in the normal direction. By carefully selecting the incident wavelength, the thickness of the SiO₂ layer on the substrate, and the geometrical size of the L pattern, the phase difference between x and y components of $|P_j\rangle$ can be adjusted to 90° or 270° . In this way, a CP state is generated from the resonator [17]. Moreover, by choosing the length and width of the arms of the L resonator, a specific GSI phase (ϕ) is imposed on the generated CP state. By taking the mirror image of the L resonator, the CP state of the opposite handedness is formed [50]. For a specific incident wavelength, we construct a pool of 16 resonators. Eight resonators make a set $\{S_i\}$ (S_1, S_2, \dots, S_8); the other eight are their mirror-imaged counterparts $\{S'_i\}$ (S'_1, S'_2, \dots, S'_8). The range of ϕ for the resonators in $\{S_i\}$ covers 0 to 2π with a step of $\pi/4$, and the same applies for that in $\{S'_i\}$. The mathematical form of the radiation from the resonator in $\{S_i\}$ ($\{S'_i\}$) can be written as $e^{i\phi_{S_i}}|R\rangle$ ($e^{i\phi_{S'_i}}|L\rangle$). The resonators within the unit cell are all selected from both pools $\{S_i\}$ and $\{S'_i\}$.

Consider the matrix representation of Eq. (4), $|k_n\rangle = \mathbf{A}|P_j\rangle$. For a given set of expected polarization states ($|k_n\rangle$), $|P_j\rangle$ can be obtained directly from $|P_j\rangle = \mathbf{A}^{-1}|k_n\rangle$ when \mathbf{A} is a reversible matrix. The number of the expected diffracted beams R_1 is associated with the diffraction order n , which relies on the ratio of the periodicity of the unit cell in x -direction D_x and the wavelength λ , i.e., $|n| \leq \frac{D_x}{\lambda}$. Yet, R_1 may not equal R_2 . To satisfy $R_1 = R_2$, some protocols are applied in selecting the resonator from the pool. The ultimate requirement is that the determinant of the corresponding matrix \mathbf{A} should be nonzero. In this paper, we apply the following etiquettes. Assume Q_1 is an even number. In the unit cell, $Q_1/2$ resonators, P_j ($j = 1, 2, \dots, Q_1/2$), are independent, whereas the rest of the resonators in the unit cell, $P_{j+Q_1/2}$ ($j = 1, 2, \dots, Q_1/2$), are affiliated to P_j by adding an additional phase. More specifically, we let the diffraction field $|P_{j+Q_1/2}\rangle$ ($j = 1, 2, \dots, Q_1/2$) possesses a phase difference π with respect to $|P_j\rangle$. It follows that all the even order diffraction fields in Eq. (4) vanish, and the output beams only have odd order. Suppose we expect to generate four beams with different states from the metasurface ($R_1 = 4$). Q_1 should be set as 4. Hence, the number of the independent resonators in the unit cell $R_2 = Q_1/2 = 4 = R_1$. Therefore \mathbf{A} is a square matrix. It is known that the diffraction efficiency, which is defined as

the ratio of the intensity of the diffracted beam to that of the incident beam, depends on the diffraction angle [51]. Usually, the high-angle diffraction has lower diffraction efficiency. For this reason, we consider four orders of diffraction with the highest diffraction efficiency, ± 1 , and ± 3 .

By taking $Q_1 = 8$ in Eq. (4), and considering four orders, ± 1 , and ± 3 , the matrix A can be written as

$$A = \frac{1}{2} \begin{bmatrix} e^{i\frac{5}{8}\pi} & e^{-i\frac{1}{8}\pi} & e^{-i\frac{7}{8}\pi} & e^{i\frac{3}{8}\pi} \\ e^{i\frac{7}{8}\pi} & e^{i\frac{5}{8}\pi} & e^{i\frac{3}{8}\pi} & e^{i\frac{1}{8}\pi} \\ e^{-i\frac{7}{8}\pi} & e^{-i\frac{5}{8}\pi} & e^{-i\frac{3}{8}\pi} & e^{-i\frac{1}{8}\pi} \\ e^{-i\frac{5}{8}\pi} & e^{i\frac{1}{8}\pi} & e^{i\frac{7}{8}\pi} & e^{-i\frac{3}{8}\pi} \end{bmatrix}. \quad (5)$$

For simplicity, here the amplitude of $|k_{-3}\rangle$, $|k_{-1}\rangle$, $|k_1\rangle$, and $|k_3\rangle$ has been normalized. Clearly, the determinant of this matrix does not equal zero. By integrating Eq. (4), and performing a matrix inversion of A [Eq. (5)], Eq. (4) becomes

$$\begin{bmatrix} |P_1\rangle \\ |P_2\rangle \\ |P_3\rangle \\ |P_4\rangle \end{bmatrix} = \frac{1}{2} \begin{bmatrix} e^{-i\frac{5}{8}\pi} & e^{-i\frac{7}{8}\pi} & e^{i\frac{7}{8}\pi} & e^{i\frac{5}{8}\pi} \\ e^{i\frac{1}{8}\pi} & e^{-i\frac{5}{8}\pi} & e^{i\frac{5}{8}\pi} & e^{-i\frac{1}{8}\pi} \\ e^{i\frac{3}{8}\pi} & e^{-i\frac{3}{8}\pi} & e^{i\frac{3}{8}\pi} & e^{-i\frac{7}{8}\pi} \\ e^{-i\frac{3}{8}\pi} & e^{-i\frac{1}{8}\pi} & e^{i\frac{1}{8}\pi} & e^{i\frac{3}{8}\pi} \end{bmatrix} \begin{bmatrix} |k_3\rangle \\ |k_1\rangle \\ |k_{-1}\rangle \\ |k_{-3}\rangle \end{bmatrix}. \quad (6)$$

Theoretically, for a given set of $|k_n\rangle$, $|P_j\rangle$ can be obtained directly from Eq. (6). Generally, the Jones vector of a specific polarization state can be expressed as $[\Gamma_n, \Delta_n e^{i\delta_n}]$, with $|\Gamma_n|^2 + |\Delta_n|^2 = 1$. For example, for LCP (RCP) state, the Jones vector is $\frac{\sqrt{2}}{2} [e^{i\frac{1}{2}}] (\frac{\sqrt{2}}{2} [e^{-i\frac{1}{2}}])$. For the horizontally (vertically) LP state, the Jones vector is $[\begin{smallmatrix} 1 \\ 0 \end{smallmatrix}]$ ($[\begin{smallmatrix} 0 \\ 1 \end{smallmatrix}]$). Here, we express $|k_n\rangle$ as the superposition of the LCP and RCP states, $|k_n\rangle = e^{i\varphi_{k_n}} (\alpha_n |L\rangle + \beta_n |R\rangle)$, where φ_{k_n} is the initial phase, which does not affect the state of polarization. For the desired state, by taking $|k_n\rangle = e^{i\varphi_{k_n}} [\Gamma_n, \Delta_n e^{i\delta_n}]$, $|L\rangle = \frac{\sqrt{2}}{2} [e^{i\frac{1}{2}}]$, $|R\rangle = \frac{\sqrt{2}}{2} [e^{-i\frac{1}{2}}]$ into the expression of $|k_n\rangle$, we obtain $\alpha_n = \frac{\sqrt{2}}{2} (\Gamma_n + \Delta_n e^{i(\delta_n - \pi/2)})$, $\beta_n = \frac{\sqrt{2}}{2} (\Gamma_n - \Delta_n e^{i(\delta_n - \pi/2)})$. In this way, for the desired polarization state, α_n and β_n can be acquired from Γ_n , Δ_n , and δ_n . For example, for the LCP (RCP) state, $\Gamma_n = \frac{\sqrt{2}}{2}$, $\Delta_n = \frac{\sqrt{2}}{2}$, $\delta_n = \frac{\pi}{2}$ ($\Gamma_n = \frac{\sqrt{2}}{2}$, $\Delta_n = \frac{\sqrt{2}}{2}$, $\delta_n = -\frac{\pi}{2}$). Accordingly, $\alpha_n = 1$, $\beta_n = 0$ ($\alpha_n = 0$, $\beta_n = 1$). Similarly, for a horizontally LP state, $\alpha_n = \beta_n = \frac{\sqrt{2}}{2}$. For a vertically LP state, $\alpha_n = -\frac{\sqrt{2}}{2}i$, $\beta_n = \frac{\sqrt{2}}{2}i$. It can be seen that for the desired output state, α_n and β_n are fixed, yet the initial phase φ_{k_n} can be arbitrarily selected. From Eq. (6), $|P_j\rangle$ can be written as the superposition of $|L\rangle$ and $|R\rangle$ ($\alpha_j |L\rangle + \beta_j |R\rangle$), where the coefficient α_j and β_j are directly determined by the value of φ_{k_n} . In our system, $|P_j\rangle$ should be the radiation from the resonators from the pools $\{S_i\}$ and $\{S'_i\}$, and always possess the form of $e^{i\phi_{S_i}} |R\rangle$ or $e^{i\phi_{S'_i}} |L\rangle$. This requires that either α_j or β_j should vanish. To obtain $|P_j\rangle$ that can be realized by the L-shaped resonators from the pool, a parameter scan of the initial phases φ_{k_n} of $|k_n\rangle$ should be made. More specifically, for the desired set of polarization states,

$$|k_n\rangle = \begin{bmatrix} e^{i\varphi_{k_3}} (\alpha_3 |L\rangle + \beta_3 |R\rangle) \\ e^{i\varphi_{k_1}} (\alpha_1 |L\rangle + \beta_1 |R\rangle) \\ e^{i\varphi_{k_{-1}}} (\alpha_{-1} |L\rangle + \beta_{-1} |R\rangle) \\ e^{i\varphi_{k_{-3}}} (\alpha_{-3} |L\rangle + \beta_{-3} |R\rangle) \end{bmatrix}.$$

α_n and β_n are known, and the initial phase of each diffracted beam φ_{k_n} scans from 0 to $15\pi/8$ with a step of $\pi/8$. Because there are four desired beams, and 16 possible values (0, $\pi/8$, $2\pi/8$, ..., $15\pi/8$) of the initial phase of each beam, the number of combinations of $|k_n\rangle$ is accordingly 16^4 . 16^4 combinations of $|k_n\rangle$ correspond to 16^4 combinations of $|P_j\rangle$. From the total 16^4 combinations of $|P_j\rangle$, we select the one that allows $|P_j\rangle$ ($j = 1, 2, 3$, and 4) being written as $e^{i\phi_{S_i}} |R\rangle$ or $e^{i\phi_{S'_i}} |L\rangle$. For example, if we expect to have $|H\rangle$, $|R\rangle$, $|V\rangle$, and $|L\rangle$ at the order of 3rd, 1st, -1st, and -3rd, respectively. When the initial phases of the four states equal to 0, $|k_n\rangle$ has the form of

$$|k_n\rangle = \begin{bmatrix} \sqrt{2}(|L\rangle + |R\rangle)/2 \\ |R\rangle \\ -\sqrt{2}i(|L\rangle - |R\rangle)/2 \\ |L\rangle \end{bmatrix}.$$

Taking $|k_n\rangle$ into Eq. (6), we obtain $|P_1\rangle = [e^{i\frac{5}{8}\pi} |L\rangle + (e^{i\frac{9}{8}\pi} + \sqrt{2}e^{i\frac{11}{8}\pi}) |R\rangle]/2$, $|P_2\rangle = [(e^{i\frac{15}{8}\pi} + \sqrt{2}e^{i\frac{13}{8}\pi}) |L\rangle + e^{i\frac{11}{8}\pi} |R\rangle]/2$, $|P_3\rangle = [e^{i\frac{7}{8}\pi} |L\rangle + (e^{i\frac{13}{8}\pi} + \sqrt{2}e^{i\frac{7}{8}\pi}) |R\rangle]/2$, $|P_4\rangle = [e^{i\frac{3}{8}\pi} + \sqrt{2}e^{i\frac{13}{8}\pi}) |L\rangle + e^{i\frac{15}{8}\pi} |R\rangle]/2$. Obviously, the retrieved $|P_j\rangle$ does not satisfy that one of α_j and β_j equals zero. Then we do the parameter scan of φ_{k_n} , and find that only when $|k_n\rangle$ has the form of

$$|k_n\rangle = \begin{bmatrix} \sqrt{2}e^{i\frac{3}{8}\pi} (|L\rangle + |R\rangle)/2 \\ e^{i\frac{7}{8}\pi} |R\rangle \\ \sqrt{2}e^{i\frac{3}{8}\pi} (|L\rangle - |R\rangle)/2 \\ e^{i\frac{15}{8}\pi} |L\rangle \end{bmatrix},$$

$|P_1\rangle = |R\rangle$, $|P_2\rangle = e^{i\frac{1}{4}\pi} |R\rangle$, $|P_3\rangle = e^{i\pi} |L\rangle$, $|P_4\rangle = e^{i\frac{1}{4}\pi} |L\rangle$. $|P_5\rangle$ - $|P_8\rangle$ can be obtained by adding $e^{i\pi}$ phase. In this way, the desired unit cell is established.

III. METASURFACE I: GENERATING TWO LP AND TWO CP STATES

In order to elucidate the process to obtain multiple beams with nonorthogonal polarization states, such as CP and LP states, from a single piece of metasurface, we set the expected states as $|L\rangle$, $|V\rangle$, $|R\rangle$, and $|H\rangle$ at -3rd, -1st, 1st, and 3rd order, respectively. By taking

$$|k_n\rangle = \begin{bmatrix} \sqrt{2}e^{i\varphi_{k_3}} (|L\rangle + |R\rangle)/2 \\ e^{i\varphi_{k_1}} |R\rangle \\ \sqrt{2}e^{i(\varphi_{k_{-1}} - \pi/2)} (|L\rangle - |R\rangle)/2 \\ e^{i\varphi_{k_{-3}}} |L\rangle \end{bmatrix}$$

into Eq. (6), and performing a parameter scan of the initial phases φ_{k_n} , we get

$$|P_j\rangle = \begin{bmatrix} |R\rangle \\ e^{i\frac{\pi}{4}} |R\rangle \\ e^{i\pi} |L\rangle \\ e^{i\frac{\pi}{4}} |L\rangle \end{bmatrix}.$$

Since the diffraction field $|P_{j+4}\rangle$ ($j = 1, 2, 3$, and 4) possesses a phase difference π than $|P_j\rangle$, the phase and the handedness of the light radiated from each resonator in the unit cell should

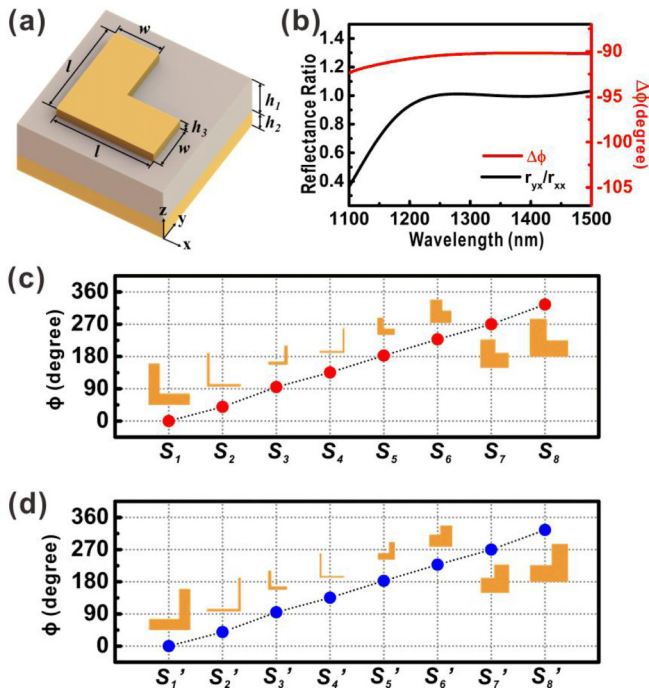


FIG. 1. The simulation results of 16 L-shaped resonators (S_1, S_2, \dots, S_8 and S_1', S_2', \dots, S_8') in PS1, where the x -polarized incident light propagates in $-z$ direction. (a) The detailed topography of the L-shaped resonator sitting on top of a SiO_2 -gold-silicon substrate. For the resonators in PS1, the thickness of the SiO_2 layer h_1 and that of the solid gold layer h_2 are 200 and 100 nm, respectively. The thickness of the gold L-shaped structure h_3 is 50 nm. The center-to-center separation of each resonator is set as 700 nm. The length l and width w of the eight resonators generating $|R\rangle$ (RCP state), $\{S_1, S_2, \dots, S_8\}$, and their mirror-imaged counterparts generating $|L\rangle$ (LCP state), $\{S_1', S_2', \dots, S_8'\}$, are listed in Table I. (b) The plot showing the simulated reflectance ratio, and phase difference of the y and x components of the reflected beam when the incident beam interacts with S_1 . (c) The simulated GSI phase ϕ added to the diffracted state from the elements in $\{S_i\}$ ($i = 1, 2, \dots, 8$). The incident wavelength is 1300 nm. (d) The simulated GSI phase ϕ added to the diffracted state from the elements in $\{S_i'\}$ ($i = 1, 2, \dots, 8$). The incident wavelength is 1300 nm.

be $|R\rangle, e^{i\frac{\pi}{4}}|R\rangle, e^{i\pi}|L\rangle, e^{i\frac{\pi}{4}}|L\rangle, e^{i\pi}|R\rangle, e^{i\frac{5\pi}{4}}|R\rangle, |L\rangle,$ and $e^{i\frac{5\pi}{4}}|L\rangle$, respectively.

The pool PS1 is designed for the x -polarized incidence with wavelength 1300 nm. Figure 1 shows the polarization and phase characteristics of the diffraction from each resonator in the sets $\{S_i\}$ and $\{S_i'\}$ of PS1, which are simulated by the finite difference time domain (FDTD) method. As indicated in Fig. 1(a), each resonator is an L-shaped gold structure sitting on top of a SiO_2 -gold-silicon substrate, with its opening pointing towards 45° (or 135°) [17]. The thickness of the SiO_2 layer h_1 and that of the solid gold layer h_2 are 200 and 100 nm, respectively. The thickness of the gold L-shaped structure h_3 is 50 nm. The center-to-center separation of each resonator is set as 700 nm. The length l and width w of the eight resonators generating $|R\rangle$ (RCP state), $\{S_1, S_2, \dots, S_8\}$, and their mirror-imaged counterparts generating $|L\rangle$ (LCP state), $\{S_1', S_2', \dots, S_8'\}$, are listed in Table I. We focus on three

TABLE I. l and w of the L-shaped structures in PS1. The center-to-center separation of the neighboring structures in the x direction is 700 nm. Each resonator diffracts a CP state with a GSI phase ϕ . The incident wavelength is 1300 nm.

$ R\rangle$	S_1	S_2	S_3	S_4	S_5	S_6	S_7	S_8
$ L\rangle$	S_1'	S_2'	S_3'	S_4'	S_5'	S_6'	S_7'	S_8'
l (nm)	500	410	235	300	220	285	345	465
w (nm)	145	40	50	30	85	150	185	210
ϕ	0	$\pi/4$	$\pi/2$	$3\pi/4$	π	$5\pi/4$	$3\pi/2$	$7\pi/4$

parameters for each resonator: the reflectance ratio of y and x components (r_{yx}/r_{xx}), the reflected phase difference between y and x components ($\Delta\phi$), and the GSI phase ϕ . r_{yx}/r_{xx} and $\Delta\phi$ determine the polarization state of the diffraction from the resonator. For a CP state, the reflectance ratio equals 1, and the phase difference equals 90° or 270° . Figure 1(b) illustrates the simulated reflectance ratio r_{yx}/r_{xx} and the phase difference between y and x components when the incident light shines on the resonators S_1 in PS1. The reflectance ratio keeps unity, and the phase of the x component is 90° advanced at 1300 nm, meaning that the resonator generates an RCP state. Figures 1(c) and 1(d) show the simulated GSI phase ϕ of the diffracted CP state from the resonators. It can be seen that the range of ϕ for the resonators in $\{S_i\}$ covers 0 to 2π with a step of $\pi/4$, and the same applies for that in $\{S_i'\}$. The simulation results in Fig. 1 indicate that upon normal illumination of an x -polarized incidence of 1300 nm, resonators in $\{S_i\}$ ($\{S_i'\}$) of PS1 generate RCP (LCP) state, and a GSI phase ϕ is introduced to the diffraction field from each resonator.

To meet the requirement that the phase and the handedness of the light radiated from each resonator in the unit cell are $|R\rangle, e^{i\frac{\pi}{4}}|R\rangle, e^{i\pi}|L\rangle, e^{i\frac{\pi}{4}}|L\rangle, e^{i\pi}|R\rangle, e^{i\frac{5\pi}{4}}|R\rangle, |L\rangle,$ and $e^{i\frac{5\pi}{4}}|L\rangle$, the resonators should be selected as $S_1, S_2, S_5', S_2', S_5, S_6, S_1', S_6'$ from PS1, as illustrated in Fig. 2(a). In this case, since the separation of resonators in the x direction is 700 nm, and the number of resonators within the unit cell is 8, D_x becomes 5600 nm. The incident wavelength is 1300 nm. It follows that $|n| \leq 4$. Because the output beams only have odd orders, the observable n is ± 1 and ± 3 . This situation means that all of the four beams $|k_{-3}\rangle, |k_{-1}\rangle, |k_1\rangle,$ and $|k_3\rangle$ can be diffracted into the free space. We emphasize here that the four generated polarization states include two CP (LCP, RCP) states and two LP (horizontal, vertical) states, which cannot be achieved so far with other approaches to the best of our knowledge.

An array of L-shaped resonator assembly on SiO_2 -gold-silicon substrate has been fabricated to verify the theoretical design, as shown in Fig. 2(b). To characterize the fabricated sample, a supercontinuum laser and a Glan-Taylor polarizer are used to generate the LP incident beam with a wavelength range of 400–2000 nm. A near-infrared fiber spectrometer (900–1600 nm) is installed on the rotation stage to measure the diffraction intensity in the ranges of -60° to -12° and 12° to 60° in the reflection mode. The region between 12° and -12° cannot be detected due to the technical restriction of the reflection mode, which is marked by two dashed lines in the angle-resolved diffraction spectrum. An achromatic

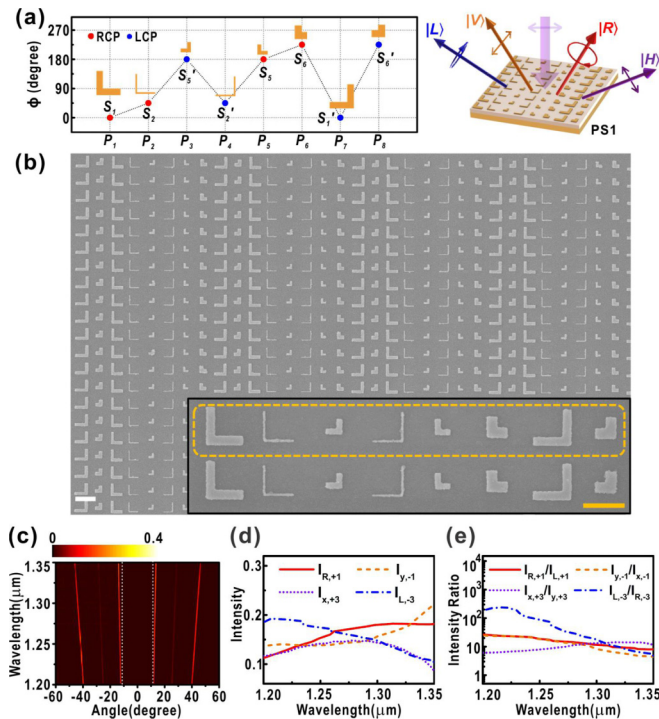


FIG. 2. (a) The plot to show the GSI phase ϕ and the handedness (represented by the red/blue dots) of each resonator in the unit cell. The resonators are selected from PS1. Four from $\{S_i\}$ and four from $\{S'_i\}$. The metasurface generates two LP and two CP states. (b) SEM micrograph of the fabricated metasurface as designed in Fig. 2(a). The inset is the enlarged SEM micrograph. The dash line box marks the unit cell. Both the white and yellow bars represent $1 \mu\text{m}$. (c) Measured angle-resolved diffraction spectra. Four bright lines represent the diffracted beams measured at different wavelength at different diffraction angles. The color bar stands for the intensity. (d) The normalized beam intensity of four diffracted beams. $I_{pol,num}$ represents the intensity of num^{th} order with pol polarization. (e) The measured light intensity ratio of each beam.

quarter-wave plate and/or a polarizer are installed in front of the detector to identify the polarization state of each diffracted beam. The angle-resolved diffraction spectrum is illustrated in Fig. 2(c). It can be seen that four diffracted beams, from left to right, correspond to -3rd , -1st , 1st , and 3rd order of diffraction, have been detected. To characterize the diffraction efficiency, we define the normalized beam intensity as the intensity of the diffracted beam and that of the incident beam, as illustrated in Fig. 2(d). At wavelength 1300 nm , the normalized intensity of the diffraction beam is 14.42% , 15.72% , 17.96% , and 14.32% , respectively, corresponding to -3rd , -1st , 1st , and 3rd order. The total intensity reaches 62.42% . Experimentally we define a parameter, the light intensity ratio, to characterize the purity of each generated state. For the LP beam, the light intensity ratio is defined as the ratio of the intensity of the investigated beam and the intensity detected with the orthogonal polarization; for the CP beam, it is defined as the ratio of the intensity of the investigated beam and that with the conjugated CP. For the ideal situation, this ratio should be infinity for a pure CP/LP state. However, in real experiments, the conjugated polarization state does not vanish completely due to defects in lithography. Consequently, this ratio usually

TABLE II. l and w of L-shaped resonators in PS2 when the center-to-center separation of the neighboring resonators has been shrunk to 400 nm . Each L-shaped resonator diffracts a CP state with a GSI phase ϕ . The incident wavelength is 1200 nm .

	S_1	S_2	S_3	S_4	S_5	S_6	S_7	S_8
$ R\rangle$	S_1	S_2	S_3	S_4	S_5	S_6	S_7	S_8
$ L\rangle$	S'_1	S'_2	S'_3	S'_4	S'_5	S'_6	S'_7	S'_8
l (nm)	230	270	310	290	150	220	160	200
w (nm)	125	125	80	30	25	20	50	105
ϕ	0	$\pi/4$	$\pi/2$	$3\pi/4$	π	$5\pi/4$	$3\pi/2$	$7\pi/4$

ends up with a large value. This suggests that each resonator in the unit cell contributes a more accurate phase and amplitude. Hence, the interaction of all the diffracted light leads to the beams with the desired polarization states. The light intensity ratio of these four beams is presented in Fig. 2(e). The intensity ratios are respectively 19.18 (-3rd order), 8.16 (-1st order), 11.78 ($+1\text{st}$ order), and 13.26 ($+3\text{rd}$ order) at 1300 nm . Figure 2(e) confirms that two CP states and two LP states have been experimentally realized.

IV. METASURFACE II: GENERATING ONE VERTICALLY LP AND ONE RCP STATES

Let us consider the rearrangement of the resonators in the unit cell. The diffraction order n requires $|n| \leq \frac{D_x}{\lambda}$. For the scenario $3\lambda < D_x < 5\lambda$, $n = \pm 1, \pm 3$ can be diffracted from the metasurface to four directions [Fig. 2(c)]. If the separation of the resonators in the unit cell has been so shrunk that $\lambda < D_x < 3\lambda$ is satisfied, then only ± 1 order of diffraction survives in the free space. This means that tuning D_x/λ is an efficient way to control the number of diffracted beams.

To diffract only two beams from the metasurface, we shrink the separation of resonators in the x direction from 700 to 400 nm . So D_x becomes 3200 nm . When we select the wavelength as 1200 nm , we have $|n| \leq 2$. It is noteworthy that once the separation of the resonators has been changed, the other parameters of the system, such as the thickness of SiO_2 layer h_1 and the geometrical size of the resonators, should be adjusted accordingly. Therefore we construct the second pool PS2 for incident wavelength 1200 nm . The thickness of the SiO_2 layer h_1 and that of the solid gold layer h_2 are selected as 110 and 100 nm , respectively. The gold L-shaped structure h_3 is set as 50 nm in thickness. The separation of each resonator is 400 nm . The length l and width w of the eight resonators generating $|R\rangle$ and their mirror-imaged counterparts generating $|L\rangle$ are listed in Table II. Figure 3(a) illustrates the simulated reflectance ratio r_{yx}/r_{xx} and the phase difference between y and x components when the incident light shines on the resonators S_1 in PS2. The reflectance ratio remains unity and the phase of the x component is 90° advanced at 1200 nm , indicating that the resonator generates the RCP state. Figures 3(b) and 3(c) are the simulated GSI phase ϕ of the diffracted CP state from the resonators in PS2. It can be seen that the range of ϕ for the resonators in $\{S_i\}$ covers 0 to 2π with a step of $\pi/4$, and the same applies for that in $\{S'_i\}$. The simulation results in Fig. 3 indicate that upon normal illumination of an x -polarized incidence with wavelength 1200 nm , resonators in $\{S_i\}$ ($\{S'_i\}$) of PS2 generate an RCP

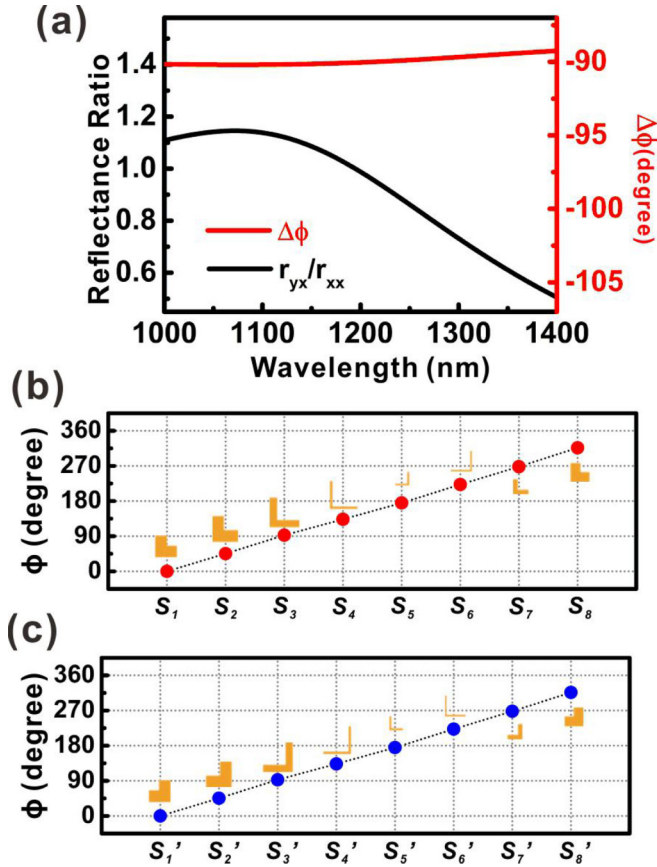


FIG. 3. The simulation results of 16 L-shaped resonators (S_1, S_2, \dots, S_8 and S_1', S_2', \dots, S_8') in PS2, where the x -polarized incident light propagates in $-z$ direction. For the resonators in PS2, the thickness of the SiO_2 layer h_1 and that of the solid gold layer h_2 are selected as 110 and 100 nm, respectively. The gold L-shaped structure h_3 is set as 50 nm. The separation of each resonator is 400 nm. The length l and width w of the eight resonators generating $|R\rangle$ and their mirror-imaged counterparts generating $|L\rangle$ are listed in Table II. (a) The plot to show the simulated reflectance ratio, and phase difference of the y and x components of the reflected beam when the incident beam interacts with S_1 . (b) The simulated GSI phase ϕ added to the diffracted state from the elements in $\{S_i\}$ ($i = 1, 2, \dots, 8$). The incident wavelength is 1200 nm. (c) The simulated GSI phase ϕ added to the diffracted state from the elements in $\{S_i'\}$ ($i = 1, 2, \dots, 8$). The incident wavelength is 1200 nm.

(LCP) state, and a GSI phase ϕ is added to the diffraction field of each resonator.

When the resonators are selected from PS2, and Q_1 is still equal to 8, $|n| \leq 2$ is always satisfied. In this paper, the diffracted beams are limited to odd orders. Hence, only two beams of ± 1 order are diffracted. The higher diffraction orders cannot be observed due to the restriction $|n| \leq \frac{D_x}{\lambda}$. In this scenario, Eq. (6) is still valid. The process of the parameter scan of the initial phases is the same as that shown in Sec. III. The only difference is that here only two states are observed, whereas the other two beams (± 3 orders) are evanescent ones [57].

Suppose that the expected nonorthogonal states at -1 st and 1 st order are $|V\rangle$ and $|R\rangle$. The evanescent beams at -3 rd and 3 rd order are $|L\rangle$ and $|H\rangle$. Hence, the mathematical form

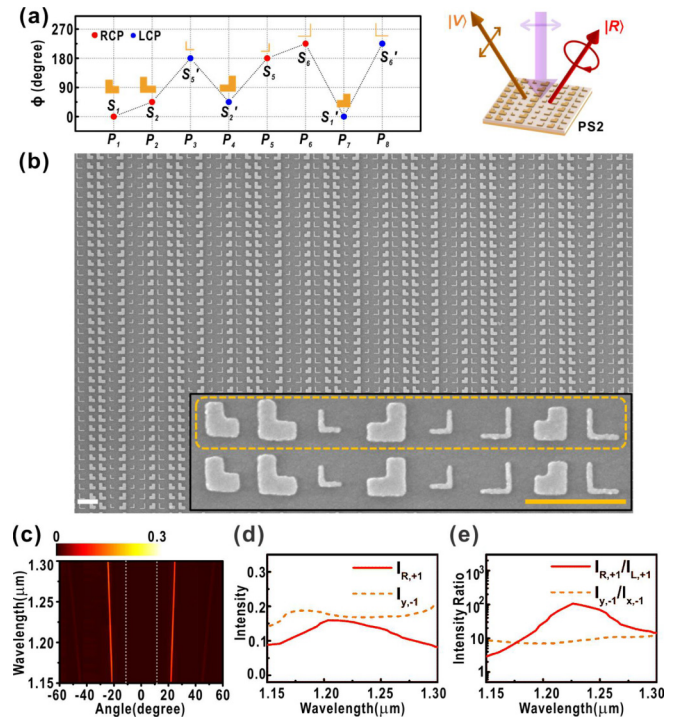


FIG. 4. (a) The plot to show the GSI phase ϕ and the handedness (represented by the red/blue dots) of each resonator in the unit cell. The resonators are selected from PS2. Four from $\{S_i\}$ and four from $\{S_i'\}$. The metasurface generates one LP and one CP state. (b) SEM micrograph of the fabricated metasurface as designed in Fig. 4(a). The inset is the enlarged SEM micrograph. The dash line box marks the unit cell. Both the white bar and yellow bar represent $1 \mu\text{m}$. (c) Measured angle-resolved diffraction spectra. Two bright lines represent the diffracted beams measured at different wavelengths at different diffraction angles. The color bar stands for the intensity. (d) The normalized beam intensity of two diffracted beams. $I_{pol,num}$ represents the intensity of num^{th} order with pol polarization. (e) The measured light intensity ratio of each beam.

of $|k_n\rangle$ is the same as that in Sec. III. It follows that these two scenarios share the same solution. The phase and the handedness of the light radiated from each resonator in the unit cell are still $|R\rangle, e^{i\frac{\pi}{4}}|R\rangle, e^{i\pi}|L\rangle, e^{i\frac{\pi}{4}}|L\rangle, e^{i\pi}|R\rangle, e^{i\frac{3\pi}{4}}|R\rangle, |L\rangle$, and $e^{i\frac{3\pi}{4}}|L\rangle$. The corresponding resonators are selected as $S_1, S_2, S_5', S_2', S_5, S_6, S_1', S_6'$ in PS2, as illustrated in Fig. 4(a). In this case, the output diffracted beams are one RCP state and one LP (vertical) state.

The metasurface diffracting CP state and other linearly polarized states, such as $\pm 45^\circ$ -LP or horizontally LP can be treated similarly. For example, when $|k_{-1}\rangle$ and $|k_1\rangle$ are respectively RCP and horizontally LP, meanwhile, the evanescent beams at -3 rd and 3 rd order are $|L\rangle$ and $|V\rangle$, the spatial sequence of the resonators [the solution of Eq. (6)] is $S_1, S_2, S_1', S_6', S_5, S_6, S_5', S_2'$. When $|k_{-1}\rangle$ and $|k_1\rangle$ are respectively RCP and -45° -LP, meanwhile, $|k_{-3}\rangle$ and $|k_3\rangle$ are LCP and $+45^\circ$ -LP, then the spatial sequence of the resonators should be selected as $S_8, S_1, S_2', S_7', S_4, S_5, S_6',$ and S_3' .

To verify the theoretical design, we fabricate the metasurface with the unit cell elements shown in Fig. 4(a), as shown in Fig. 4(b). Figure 4(c) illustrates the angle-resolved diffraction spectrum of the metasurface, where two diffraction beams

belong to 1st and -1 st order, respectively. The measured normalized beam intensity of the two diffraction orders is shown in Fig. 4(d). At wavelength 1200nm, the normalized intensity of the diffracted beam is 18.16% and 15.94%, respectively, corresponding to -1 st and 1st order. The total normalized intensity reaches 34.1%. The light intensity ratio of the two beams is shown in Fig. 4(e). At 1200 nm, the intensity ratios of the diffracted beams are respectively 7.03 and 33.59. Figure 4 confirms that we have indeed experimentally realized the theoretical design.

V. METASURFACE III: GENERATING ONE HORIZONTALLY AND ONE VERTICALLY LP STATES

In Sec. IV, there are eight resonators in the unit cell, and four are independent ($R_2 = Q_1/2 = 4$). To satisfy A is a reversible matrix, the number of diffracted beams should satisfy $R_1 = R_2 = 4$. Hence, apart from the two desired states, two evanescent beams are taken into consideration. In this Section, we provide another solution about two diffracted beams. We follow the same protocol as mentioned in Sec. II, that the diffraction field $P_{j+Q_1/2}$ ($j = 1, 2, \dots, Q_1/2$) possesses a phase difference π with respect to P_j . Q_1 and R_2 satisfy $R_2 = Q_1/2$. Here, we only consider the two desired beams ($R_1 = 2$). To satisfy A is square, $R_2 = R_1 = 2$, $Q_1 = 4$. This means that there are only four resonators in the unit cell. By taking $Q_1 = 4$ in Eq. (4) considering two orders, ± 1 , and performing a matrix inversion, Eq. (4) becomes

$$\begin{bmatrix} |P_1\rangle \\ |P_2\rangle \end{bmatrix} = \frac{\sqrt{2}}{2} \begin{bmatrix} e^{-i\frac{3}{4}\pi} & e^{i\frac{3}{4}\pi} \\ e^{-i\frac{1}{4}\pi} & e^{i\frac{1}{4}\pi} \end{bmatrix} \begin{bmatrix} |k_1\rangle \\ |k_{-1}\rangle \end{bmatrix}. \quad (7)$$

For the given set of $|k_n\rangle$, $|P_j\rangle$ is obtained directly from Eq. (7). Then, the parameter scan is the same as that described in Sec. II.

Here we focus on another example of the generation of two beams with the resonators selected from PS2. When the resonators are selected from PS2, and Q_1 is equal to 4, $|n| \leq 2$ is still satisfied. Hence, only two beams of ± 1 orders are diffracted. Suppose that the expected states of 1st and -1 st order are $|H\rangle$ and $|V\rangle$. By taking $|k_n\rangle = \begin{bmatrix} \sqrt{2}e^{i\varphi_{k_1}}(|L\rangle + |R\rangle)/2 \\ \sqrt{2}e^{i(\varphi_{k_{-1}} - \pi/2)}(|L\rangle - |R\rangle)/2 \end{bmatrix}$ into Eq. (7) and performing a parameter scan of the initial phases φ_{k_n} , we obtain $|P_j\rangle = \begin{bmatrix} |R\rangle \\ e^{i\frac{\pi}{2}}|L\rangle \end{bmatrix}$. Since the diffraction field P_{j+2} ($j = 1, 2$) possesses a phase difference π with respect to P_j , it follows that the phase and the handedness of the light radiated from each resonator in the unit cell should be $|R\rangle$, $e^{i\frac{\pi}{2}}|L\rangle$, $e^{i\pi}|R\rangle$, $e^{i\frac{3\pi}{2}}|L\rangle$, respectively. This means that the resonators in the unit cell should be selected as S_1, S_3', S_5, S_7' , as illustrated in Fig. 5(a).

We fabricate the metasurface with the unit cell as S_1, S_3', S_5 , and S_7' , as illustrated in Fig. 5(b). Figure 5(c) shows the angle-resolved diffraction spectrum of the metasurface, where two diffraction beams are clearly demonstrated. The measured normalized beam intensity of two diffraction orders is shown in Fig. 5(d). At 1200 nm, the normalized intensity of the diffracted beam is 33.59% (-1 st order) and 24.08% ($+1$ st order). The total intensity in these two directions is 57.67%. The light intensity ratio of the two beams is shown in Fig. 5(e). The two ratios are respectively 21.50 and 8.07.

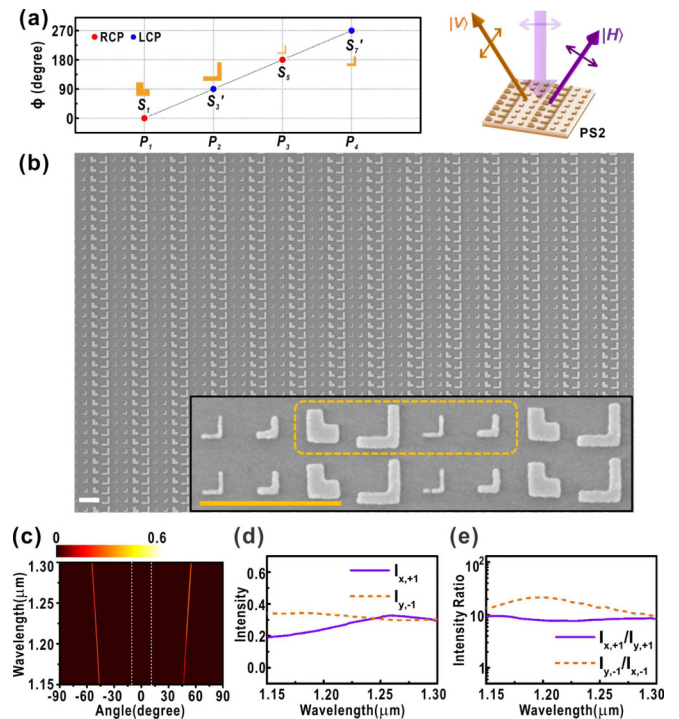


FIG. 5. (a) The plot to show the GSI phase ϕ and the handedness (represented by the red/blue dots) of each resonator in the unit cell. The resonators are selected from PS2. Two from $\{S_j\}$ and two from $\{S'_j\}$. The metasurface generates one vertically and one horizontally LP state. (b) SEM micrograph of the fabricated metasurface as designed in Fig. 5(a). The inset is the enlarged SEM micrograph. The dash line box marks the unit cell. Both the white and yellow bars represent $1 \mu\text{m}$. (c) Measured angle-resolved diffraction spectra. Two bright lines represent the diffracted beams measured at different wavelength at different diffraction angles. The color bar stands for the intensity. (d) The normalized beam intensity of two diffracted beams. $I_{pol,num}$ represents the intensity of num^{th} order with pol polarization. (e) The measured light intensity ratio of each beam.

Figure 5 indicates that we have indeed experimentally realized the theoretical design.

VI. METASURFACE IV: GENERATING AN RCP STATE ONLY

Now let us consider the unique scenario where only one diffracted beam is generated from the metasurface. Suppose that the diffracted order is $+1$. The resonators are selected from PS2, and there are eight resonators within the unit cell, where $\lambda < D_x < 3\lambda$ is satisfied. Only ± 1 orders of diffraction survive. The beams of other diffraction orders are evanescent due to the restriction $|n| \leq \frac{D_x}{\lambda}$. When $|k_1\rangle$ is set as RCP, by taking

$$|k_n\rangle = \begin{bmatrix} 0 \\ e^{i\varphi_{k_1}}|R\rangle \\ 0 \\ 0 \end{bmatrix}$$

into Eq. (6) and performing a scan of φ_{k_1} , we find that the resonators in the unit cell should be selected as $S_1, S_2, S_3, S_4, S_5, S_6, S_7$, and S_8 , as illustrated in Fig. 6(a).

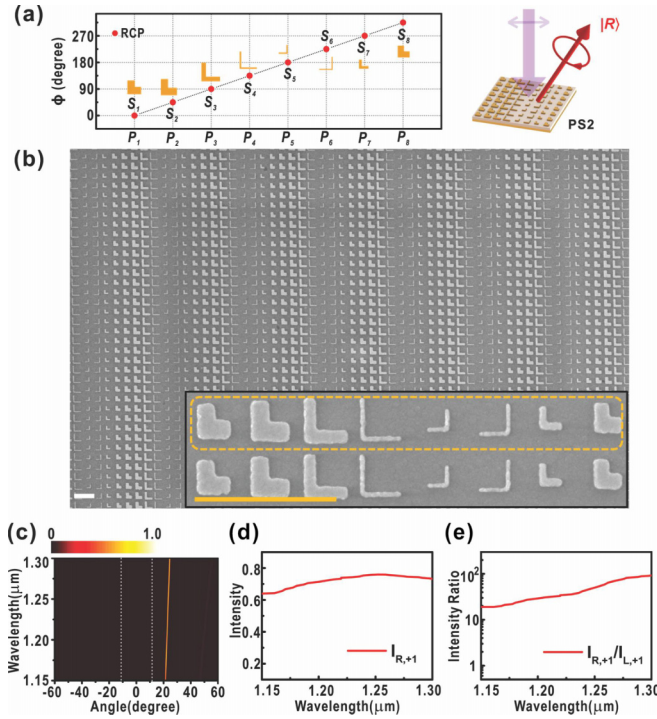


FIG. 6. (a) The plot to show the GSI phase ϕ and the handedness (represented by the red dots) of each resonator in the unit cell. The resonators are all selected from $\{S_i\}$ of PS2. The metasurface generates one RCP state. (b) SEM micrograph of the fabricated metasurface as designed in Fig. 6(a). The inset is the enlarged SEM micrograph. The dash line box marks the unit cell. Both the white bar and yellow bar represent $1 \mu\text{m}$. (c) Measured angle-resolved diffraction spectra. The bright line represents the diffracted beam measured at different wavelength at different diffraction angles. The color bar stands for the intensity. (d) The normalized beam intensity of the diffracted beams. $I_{pol,num}$ represents the intensity of num^{th} order with pol polarization. (e) The measured light intensity ratio of the beam.

To verify the theoretical design, we fabricate the metasurface with the unit cell elements shown in Fig. 6(a), as illustrated in Fig. 6(b). The angle-resolved diffraction spectrum in Fig. 6(c) shows the generated one diffraction beam. The measured normalized beam intensity is shown in Fig. 6(d). At 1200 nm, the normalized intensity of the diffracted beam at the +1st order is 71.38%. The light intensity ratio in Fig. 6(e) shows that at 1200 nm, the intensity ratio of the diffracted beam is 29.09. Figure 6 shows that we have indeed experimentally realized the theoretical design.

With the matrix inversion approach, the metasurface diffracting one beam with other polarizations can also be designed. For example, if $|k_1\rangle$ is set as horizontally LP, we take

$$|k_n\rangle = \begin{bmatrix} 0 \\ \sqrt{2}e^{i\varphi_{k_1}}(|L\rangle + |R\rangle)/2 \\ 0 \\ 0 \end{bmatrix}$$

into Eq. (6). It follows that $|P_j\rangle$ has the form of $\sqrt{2}[e^{i\Phi_1}|L\rangle + e^{i\Phi_2}|R\rangle]/2$. This means that $|P_j\rangle$ contain both RCP and LCP

components, which cannot be generated from the pools $\{S_i\}$ and $\{S'_i\}$. As a compromise approach, we introduce the beam of -3rd order, which is evanescent due to $|n| \leq \frac{D_x}{\lambda}$. Suppose this evanescent beam at -3rd order is $|V\rangle$. By taking

$$|k_n\rangle = \begin{bmatrix} 0 \\ \sqrt{2}e^{i\varphi_{k_1}}(|L\rangle + |R\rangle)/2 \\ 0 \\ \sqrt{2}e^{i(\varphi_{k_3} - \pi/2)}(|L\rangle - |R\rangle)/2 \end{bmatrix}$$

into Eq. (6) and performing a scan of φ_{k_1} and φ_{k_3} , the spatial sequence of the resonators (the solution of Eq. (6) is $S_1, S_2', S_3, S_4', S_5, S_6', S_7, S_8'$. If $|k_1\rangle$ is set as 45°-LP , similarly we introduce the states at -3rd order as -45°-LP . It follows that

$$|k_n\rangle = \begin{bmatrix} 0 \\ \sqrt{2}e^{i(\varphi_{k_1} - \pi/4)}(|L\rangle + i|R\rangle)/2 \\ 0 \\ \sqrt{2}e^{i(\varphi_{k_3} + 3\pi/4)}(|L\rangle - i|R\rangle)/2 \end{bmatrix}.$$

By taking $|k_n\rangle$ into Eq. (6) and scan for the parameters of φ_{k_1} and φ_{k_3} , we find that the spatial sequence of the resonators [the solution of Eq. (6)] should be $S_1, S_8', S_3, S_2', S_5, S_4', S_7$, and S_6' .

VII. DISCUSSION

In our design, the number of the diffraction beams is determined by both the diffraction order n and the selection of the resonators within the unit cell. The diffraction order n satisfies $|n| \leq \frac{D_x}{\lambda}$. Meanwhile, the selection of the resonators within the unit cell can lead to the extinction of the electric field in some diffraction orders. In Sec. III–V, because $|P_j\rangle$ and $|P_{j+Q_1/2}\rangle$ ($j = 1, 2, \dots, Q_1/2$) possess a phase difference of π , only odd orders of the output beams survive. When $3\lambda < D_x < 5\lambda$, $n = \pm 1, \pm 3$ can be diffracted from the metasurface to four different directions (metasurface I). In the scenario of $\lambda < D_x < 3\lambda$, $|n| < 2$. This means that only two beams with $\pm 1\text{st}$ diffraction order can be observed (metasurfaces II and III). With a specific sequence, there is only one beam diffracted from the metasurface (metasurface IV).

It should be emphasized that the spatial sequence of the resonators in the unit cell affects both the output states and the number of the diffracted beams. As an example, let us take the unit cell consisting of $S_1, S_2, S_5', S_2', S_5, S_6, S_1',$ and S_6' from PS1. The eight resonators in the unit cell may generate $384 (C_8^1 C_6^1 C_4^1 C_2^1)$ combinations, all satisfying that the diffraction field $|P_j\rangle$ and $|P_{j+4}\rangle$ ($j = 1, 2, 3,$ and 4) possess a phase difference π . The output beams of the 384 combinations are limited to $\pm 1,$ and ± 3 orders. Furthermore, since the unit cell is periodically arranged in the metasurface, once the resonators within the unit cell are sequentially permuted, macroscopically, the output states resume. Therefore the number of really independent combinations will be $1/8$ of 384. Let us take the sequence $S_1, S_2, S_5', S_2', S_5, S_6, S_1',$ and S_6' as an example. Considering sequential permutation of the elements in the unit cell, seven other sequences are generating the same output states, such as $S_2, S_5', S_2', S_5, S_6, S_1', S_6', S_1; S_5', S_2', S_5, S_6, S_1', S_6', S_1, S_2;$ and $S_2', S_5, S_6, S_1', S_6', S_1, S_2, S_5',$ etc. It follows that the number of independent combinations is reduced to 48 ($384/8$). By taking each of 48 combinations

to Eq. (4), we find that eight combinations generate two CP (LCP, RCP) states and two LP (horizontal, vertical) states, eight generate three LP states (two $+45^\circ$ -LP, one -45° -LP or two -45° -LP, one $+45^\circ$ -LP), and the rest of 32 combinations generate elliptical polarization. For example, when the spatial sequence of the resonators is selected as $S_1, S_2, S_1', S_6', S_5, S_6, S_5', S_2'$, the output states will be LCP, horizontally LP, RCP, and vertically LP, corresponding to the diffraction order $-3, -1, +1, +3$, respectively. If the spatial sequence of the resonators becomes $S_5, S_2, S_5', S_6', S_1, S_6, S_1', S_2'$, the output states become RCP, vertically LP, LCP, and horizontally LP instead. It is noteworthy that there are eight combinations that generate only three output beams because of the extinction of the electric field at one of ± 1 , and ± 3 orders. For example, when the sequence is selected as $S_1, S_2, S_5', S_6', S_5, S_6, S_1', S_2', +45^\circ$ -LP, -45° -LP, $+45^\circ$ -LP are diffracted from -1 st, 1 st, 3 rd orders, respectively. When the sequence is changed to $S_1, S_2, S_1', S_2', S_5, S_6, S_5', S_6', -45^\circ$ -LP, $+45^\circ$ -LP, -45° -LP are diffracted from -1 st, 1 st, 3 rd order. Therefore we conclude that by tuning the spatial sequence of the resonators in the unit cell, both the number of the output beams and the type of output polarization states can be adjusted.

VIII. CONCLUSION

Simultaneous generation of multiple polarization states, an important process in quantum information, can be realized with a single piece of metasurface made of L-shaped

resonators with different arm width and length. Each resonator generates an add-up phase in diffraction, which is determined by its geometrical features. With such a metasurface, an assembly of different polarization states, such as LCP, RCP, horizontally, and vertically LP states, can be simultaneously generated in different diffraction orders. The number and the propagation direction of the diffraction beams can be accurately modulated by selecting the geometrical feature, separation, and spatial order of the resonators in the unit cell of the metasurface. Here we have demonstrated a new perspective in generating one, two, or four diffraction beams with specific polarization states with one piece of the specially designed metasurface. This work demonstrates the substantial possibility of replacing bulky and heavy traditional optical components in nanophotonic device applications and promoting the development of integrated optics and information technology.

ACKNOWLEDGMENTS

The authors acknowledge one of the anonymous referees for Ref. [50], who reminded us to use the Jones matrix to describe the diffraction process. With this approach, the theoretical part becomes much easier to follow. We also acknowledge the funding support from the National Key R&D Program of China (2020YFA0211300, 2017YFA0303702) and the National Natural Science Foundation of China (Grant Nos. 11634005, 11974177, and 61975078).

- [1] T. Minamikawa, Y.-D. Hsieh, K. Shibuya, E. Hase, Y. Kaneoka, S. Okubo, H. Inaba, Y. Mizutani, H. Yamamoto, T. Iwata, and T. Yasui, Dual-comb spectroscopic ellipsometry, *Nat. Commun.* **8**, 610 (2017).
- [2] A. J. Rogers, Polarization-optical time domain reflectometry: A technique for the measurement of field distributions, *Appl. Opt.* **20**, 1060 (1981).
- [3] P. F. Kerr, *Optical Mineralogy* (McGraw-Hill, New York, 1977).
- [4] K. Perraut-Rousselet, F. Vakili, and D. Mourard, Polarization effects in stellar interferometry, *Opt. Eng.* **35**, 10 (1996).
- [5] J. E. Solomon, Polarization imaging, *Appl. Opt.* **20**, 1537 (1981).
- [6] U. Ullah, I. B. Mabrouk, and S. Koziel, Enhanced-performance circularly polarized MIMO antenna with polarization/pattern diversity, *IEEE Access* **8**, 11887 (2020).
- [7] N. Gisin, G. Ribordy, W. Tittel, and H. Zbinden, Quantum cryptography, *Rev. Mod. Phys.* **74**, 145 (2002).
- [8] P. Meystre and M. Sargent, *Elements of Quantum Optics* (Springer, New York, 2007).
- [9] H. Takenaka, A. Carrasco-Casado, M. Fujiwara, M. Kitamura, M. Sasaki, and M. Toyoshima, Satellite-to-ground quantum-limited communication using a 50-kg-class microsatellite, *Nat. Photon.* **11**, 502 (2017).
- [10] S.-K. Liao, W.-Q. Cai, W.-Y. Liu, L. Zhang, Y. Li, J.-G. Ren, J. Yin, Q. Shen, Y. Cao, Z.-P. Li, F.-Z. Li, X.-W. Chen, L.-H. Sun, J.-J. Jia, J.-C. Wu, X.-J. Jiang, J.-F. Wang, Y.-M. Huang, Q. Wang, Y.-L. Zhou *et al.*, Satellite-to-ground quantum key distribution, *Nature (London)* **549**, 43 (2017).
- [11] P. Kok, W. J. Munro, K. Nemoto, T. C. Ralph, J. P. Dowling, and G. J. Milburn, Linear optical quantum computing with photonic qubits, *Rev. Mod. Phys.* **79**, 135 (2007).
- [12] J. L. O'Brien, Optical quantum computing, *Science* **318**, 1567 (2007).
- [13] D. Tiarks, S. Schmidt-Eberle, T. Stolz, G. Rempe, and S. Dürr, A photon-photon quantum gate based on Rydberg interactions, *Nat. Phys.* **15**, 124 (2019).
- [14] H.-T. Chen, A. J. Taylor, and N. Yu, A review of metasurfaces: physics and applications, *Rep. Prog. Phys.* **79**, 076401 (2016).
- [15] P. Cheben, R. Halir, J. H. Schmid, H. A. Atwater, and D. R. Smith, Subwavelength integrated photonics, *Nature (London)* **560**, 565 (2018).
- [16] N. Yu, P. Genevet, M. A. Kats, F. Aieta, J.-P. Tetienne, F. Capasso, and Z. Gaburro, Light propagation with phase discontinuities: generalized laws of reflection and refraction, *Science* **334**, 333 (2011).
- [17] S.-C. Jiang, X. Xiong, Y.-S. Hu, Y.-H. Hu, G.-B. Ma, R.-W. Peng, C. Sun, and M. Wang, Controlling the Polarization State of Light with a Dispersion-Free Metastructure, *Phys. Rev. X* **4**, 021026 (2014).
- [18] R. H. Fan, Y. Zhou, X.-P. Ren, R.-W. Peng, S.-C. Jiang, D.-H. Xu, X. Xiong, X.-R. Huang, and M. Wang, Freely tunable broadband polarization rotator for terahertz waves, *Adv. Mater.* **27**, 1201 (2015).
- [19] A. Arbabi, Y. Horie, M. Bagheri, and A. Faraon, Dielectric metasurfaces for complete control of phase and polarization

- with subwavelength spatial resolution and high transmission, *Nat. Nanotechnol.* **10**, 937 (2015).
- [20] Z. H. Wang, S.-C. Jiang, X. Xiong, R.-W. Peng, and M. Wang, Generation of equal-intensity coherent optical beams by binary geometrical phase on metasurface, *Appl. Phys. Lett.* **108**, 261107 (2016).
- [21] P. C. Wu, J.-W. Chen, C.-W. Yin, Y.-C. Lai, T. L. Chung, C. Y. Liao, B. H. Chen, K.-W. Lee, C.-J. Chuang, C.-M. Wang, and D. P. Tsai, Visible metasurfaces for on-chip polarimetry, *ACS Photonics* **5**, 2568 (2018).
- [22] K. Wang, J. G. Titchener, S. S. Kruk, L. Xu, H.-P. Chung, M. Parry, I. I. Kravchenko, Y.-H. Chen, A. S. Solntsev, Y. S. Kivshar, D. N. Neshev, and A. A. Sukhorukov, Quantum metasurface for multiphoton interference and state reconstruction, *Science* **361**, 1104 (2018).
- [23] T. Stav, A. Faerman, E. Maguid, D. Oren, V. Kleiner, E. Hasman, and M. Segev, Quantum entanglement of the spin and orbital angular momentum of photons using metamaterials, *Science* **361**, 1101 (2018).
- [24] Z. Wu, Y. Ra'di, and A. Grbic, Tunable Metasurfaces: A Polarization Rotator Design, *Phys. Rev. X* **9**, 011036 (2019).
- [25] H. Ren, G. Briere, X. Fang, P. Ni, R. Sawant, S. Héron, S. Chenot, S. Vézian, B. Damilano, V. Brändli, S. A. Maier, and P. Genevet, Metasurface orbital angular momentum holography, *Nat. Commun.* **10**, 2986 (2019).
- [26] C.-C. Chang, Z. Zhao, D. Li, A. J. Taylor, S. Fan, and H.-T. Chen, Broadband Linear-to-Circular Polarization Conversion Enabled by Birefringent off-Resonance Reflective Metasurfaces, *Phys. Rev. Lett.* **123**, 237401 (2019).
- [27] Y. Bao, J. Ni, and C.-W. Qiu, A minimalist single-layer metasurface for arbitrary and full control of vector vortex beams, *Adv. Mater.* **32**, 1905659 (2020).
- [28] Q. Ma, Q. R. Hong, G. D. Bai, H. B. Jing, R. Y. Wu, L. Bao, Q. Cheng, and T. J. Cui, Editing Arbitrarily Linear Polarizations Using Programmable Metasurface, *Phys. Rev. Appl.* **13**, 021003(R) (2020).
- [29] Z. Shi, A. Y. Zhu, Z. Li, Y.-W. Huang, W. T. Chen, C.-W. Qiu, and F. Capasso, Continuous angle-tunable birefringence with freedom metasurfaces for arbitrary polarization conversion, *Sci. Adv.* **6**, eaba3367 (2020).
- [30] L. Deng, J. Deng, Z. Guan, J. Tao, Y. Chen, Y. Yang, D. Zhang, J. Tang, Z. Li, Z. Li, S. Yu, G. Zheng, H. Xu, C.-W. Qiu, and S. Zhang, Malus-metasurface-assisted polarization multiplexing, *Light Sci. Appl.* **9**, 101 (2020).
- [31] L. Li, Z. Liu, X. Ren, S. Wang, V.-C. Su, M.-K. Chen, C. H. Chu, H. Y. Kuo, B. Liu, W. Zang, G. Guo, L. Zhang, Z. Wang, S. Zhu, and D. P. Tsai, Metalens-array-based high-dimensional and multiphoton quantum source, *Science* **368**, 1487 (2020).
- [32] H. Ren, X. Fang, J. Jang, J. Bürger, J. Rho, and S. A. Maier, Complex-amplitude metasurface-based orbital angular momentum holography in momentum space, *Nat. Nanotechnol.* **15**, 948 (2020).
- [33] S. Lung, K. Wang, K. Z. Kamali, J. Zhang, M. Rahmani, D. N. Neshev, and A. A. Sukhorukov, Complex-birefringent dielectric metasurfaces for arbitrary polarization-pair transformations, *ACS Photonics* **7**, 3015 (2020).
- [34] Q. Fan, M. Liu, C. Zhang, W. Zhu, Y. Wang, P. Lin, F. Yan, L. Chen, H. J. Lezec, Y. Lu, A. Agrawal, and T. Xu, Independent Amplitude Control of Arbitrary Orthogonal States of Polarization Via Dielectric Metasurfaces, *Phys. Rev. Lett.* **125**, 267402 (2020).
- [35] A. H. Dorrah, N. A. Rubin, A. Zaidi, M. Tamagnone, and F. Capasso, Metasurface optics for on-demand polarization transformations along the optical path, *Nat. Photon.* **15**, 287 (2021).
- [36] M. J. Escuti, J. Kim, and M. W. Kudenov, Controlling light with geometric-phase holograms, *Opt. Photonics News* **27**, 22 (2016).
- [37] S. Pancharatnam, Generalized theory of interference and its applications, *Proc. Indian Acad. Sci. A* **44**, 398 (1956).
- [38] M. V. Berry, Quantal phase factors accompanying adiabatic changes, *Proc. Roy. Soc. Lond. A* **392**, 45 (1984).
- [39] G. Zheng, H. Mühlenbernd, M. Kenney, G. Li, T. Zentgraf, and S. Zhang, Metasurface holograms reaching 80% efficiency, *Nat. Nanotechnol.* **10**, 308 (2015).
- [40] A. Shaltout, J. Liu, A. Kildishev, and V. Shalaev, Photonic spin Hall effect in gap-plasmon metasurfaces for on-chip chiroptical spectroscopy, *Optica* **2**, 860 (2015).
- [41] M. Khorasaninejad, W. T. Chen, R. C. Devlin, J. Oh, A. Y. Zhu, and F. Capasso, Metalenses at visible wavelengths: diffraction-limited focusing and subwavelength resolution imaging, *Science* **352**, 1190 (2016).
- [42] P. C. Wu, W.-Y. Tsai, W. T. Chen, Y.-W. Huang, T.-Y. Chen, J.-W. Chen, C. Y. Liao, C. H. Chu, G. Sun, and D. P. Tsai, Versatile polarization generation with an aluminum plasmonic metasurface, *Nano. Lett.* **17**, 445 (2017).
- [43] D. Wen, F. Yue, C. Zhang, X. Zang, H. Liu, W. Wang, and X. Chen, Plasmonic metasurface for optical rotation, *Appl. Phys. Lett.* **111**, 023102 (2017).
- [44] W. T. Chen, A. Y. Zhu, V. Sanjeev, M. Khorasaninejad, Z. Shi, E. Lee, and F. Capasso, A broadband achromatic metalens for focusing and imaging in the visible, *Nat. Nanotechnol.* **13**, 220 (2018).
- [45] S. Wang, P. C. Wu, V.-C. Su, Y.-C. Lai, M.-K. Chen, H. Y. Kuo, B. H. Chen, Y. H. Chen, T.-T. Huang, J.-H. Wang, R.-M. Lin, C.-H. Kuan, T. Li, Z. Wang, S. Zhu, and D. P. Tsai, A broadband achromatic metalens in the visible, *Nat. Nanotechnol.* **13**, 227 (2018).
- [46] J. Li, S. Kamin, G. Zheng, F. Neubrech, S. Zhang, and N. Liu, Addressable metasurfaces for dynamic holography and optical information encryption, *Sci. Adv.* **4**, eaar6768 (2018).
- [47] P. K. Jha, N. Shitrit, X. Ren, Y. Wang, and X. Zhang, Spontaneous Exciton Valley Coherence in Transition Metal Dichalcogenide Monolayers Interfaced with an Anisotropic Metasurface, *Phys. Rev. Lett.* **121**, 116102 (2018).
- [48] M. Jia, Z. Wang, H. Li, X. Wang, W. Luo, S. Sun, Y. Zhang, Q. He, and L. Zhou, Efficient manipulations of circularly polarized terahertz waves with transmissive metasurfaces, *Light Sci. Appl.* **8**, 16 (2019).
- [49] P. Georgi, M. Massaro, K.-H. Luo, B. Sain, N. Montaut, H. Herrmann, T. Weiss, G. Li, C. Silberhorn, and T. Zentgraf, Metasurface interferometry toward quantum sensors, *Light Sci. Appl.* **8**, 70 (2019).
- [50] Y.-J. Gao, X. Xiong, Z. Wang, F. Chen, R.-W. Peng, and M. Wang, Simultaneous Generation of Arbitrary Assembly of Polarization States with Geometrical-Scaling-Induced Phase Modulation, *Phys. Rev. X* **10**, 031035 (2020).
- [51] E. Hecht, *Optics* (Pearson Education, Harlow, United Kingdom, 2013).

- [52] J. P. Balthasar Mueller, N. A. Rubin, R. C. Devlin, B. Groever, and F. Capasso, Metasurface Polarization Optics: Independent Phase Control of Arbitrary Orthogonal States of Polarization, *Phys. Rev. Lett.* **118**, 113901 (2017).
- [53] R. C. Devlin, A. Ambrosio, N. A. Rubin, J. P. Balthasar Mueller, and F. Capasso, Arbitrary spin-to-orbital angular momentum conversion of light, *Science* **358**, 896 (2017).
- [54] G. D. Bai, Q. Ma, R. Q. Li, J. Mu, H. B. Jing, L. Zhang, and T. J. Cui, Spin-Symmetry Breaking Through Metasurface Geometric Phases, *Phys. Rev. Applied* **12**, 044042 (2019).
- [55] Y. Yuan, S. Sun, Y. Chen, K. Zhang, X. Ding, B. Ratni, Q. Wu, S. N. Burokur, and C.-W. Qiu, A fully phase-modulated metasurface as an energy-controllable circular polarization router, *Adv. Sci.* **7**, 2001437 (2020).
- [56] Y. Yuan, K. Zhang, B. Ratni, Q. Song, X. Ding, Q. Wu, S. N. Burokur, and P. Genevet, Independent phase modulation for quadruplex polarization channels enabled by chirality-assisted geometric-phase metasurfaces, *Nat. Commun.* **11**, 4186 (2020).
- [57] E. G. Loewen and E. Popov, *Diffraction Gratings and Applications* (Marcel Dekker, New York, 1997).